Available online at www.sciencedirect.com
SCIENCE DIRECT®
Biochemical and Biophysical Research Communications 330 (2005) 172–177
BBRC
www.elsevier.com/locate/ybbrc

Localization of AQP5/AQP8 chimeras in MDCK-II cells: Exchange of the N- and C-termini

Robert B. Wellner [a], Ana P. Cotrim [a], Sohee Hong [b], William D. Swaim [a], Bruce J. Baum [a,*]

[a] *Gene Transfer Section, Gene Therapy and Therapeutics Branch, National Institute of Dental and Cranciofacial Research, National Institutes of Health, DHHS, Bethesda, MD 20892, USA*
[b] *Receptors and Signal Transduction Section, Oral Infection and Immunity Branch, National Institute of Dental and Cranciofacial Research, National Institutes of Health, DHHS, Bethesda, MD 20892, USA*

Received 16 February 2005

Abstract

AQP5 and AQP8 possess targeting/retention motifs which mediate their localization to the apical and basolateral membranes, respectively, of polarized MDCK-II cells. As targeting/retention motifs have been localized to the N- or C-termini of other AQPs, we sought the location of such motifs in AQPs 5 and 8 by exchanging their corresponding N- or C-termini and examining the expression, localization, and function of the resultant chimeras. We did not detect the expression of constructs in which the C-terminus of AQP5 was replaced by the C-terminus of AQP8. Substitution of the N-terminus of AQP8 for the N-terminus of AQP5 generated a construct which was trapped intracellularly and did not significantly facilitate transepithelial fluid movement. In contrast, modifications of the N- and C-termini of AQP8 were better tolerated. Substitution of either AQP8 terminus by the corresponding AQP5 terminus generated constructs which localized to basolateral membranes and facilitated transepithelial fluid movement. Our results suggest that, unlike the other AQP targeting/retention signals reported thus far, an AQP8 basolateral targeting/retention motif might reside between the two cytosolic termini.
Published by Elsevier Inc.

Keywords: Aquaporin; Protein sorting; Apical membrane; Basolateral membrane

The aquaporins (AQPs) are a family of polytopic membrane proteins that facilitate the movement of water and, in some cases, select small molecules (e.g., glycerol, urea) or ions [1] across membrane barriers in response to an osmotic gradient (for general reviews on AQPs see [2–4]). In membranes, the AQPs exist as homotetramers, with each monomer containing a selective pore. The monomers are composed of six membrane-spanning domains linked by five loops. The N- and C-termini reside in the cytoplasm. An hourglass model depicting AQP1 topology has been described [2].

AQPs localize to apical, basolateral, or both domains of epithelial plasma membranes. The localization of AQPs to specific plasma membrane domains involves the recognition of targeting/retention signals embedded in AQP structures by components of the cellular protein sorting machinery [5,6]. Knowledge of targeting/retention signals is important as these signals can be used to help identify interacting components of the protein localization machinery, and to direct proteins to appropriate membrane domains for therapeutic purposes. Aberrant localization of membrane proteins has been linked to human disease [7–10].

Previously we reported that AQP5 and AQP8 localize to apical and basolateral membranes, respectively, in polarized MDCK-II cells grown on polycarbonate

* Corresponding author. Fax: +1 301 402 1715.
E-mail address: BBaum@dir.nidcr.nih.gov (B.J. Baum).

0006-291X/$ - see front matter. Published by Elsevier Inc.
doi:10.1016/j.bbrc.2005.02.146

membranes [11]. We have been interested in identifying the regions of AQP5 and AQP8 encoding apical and basolateral localization information, respectively. Because localization signals have been reported to occur in the cytosolic tails of AQP2 [12], AQP4 [13], and other polytopic membrane proteins [5], we exchanged corresponding N- and C-termini between AQP5 and AQP8, and examined the expression, function, and localization of the resultant chimeras.

Materials and methods

Expression constructs. The pTRE.AQP5 [11], pTRE.AQP8 [11], and pACCMVrAQP8 [14] constructs were described previously. All modifications of AQP5 and AQP8 cDNA reported here were made using these plasmid constructs and an Advantage HF PCR Kit from Clontech. Predictions of parental and modified AQP membrane topologies and molecular weights were obtained using: (i) GeneTool (ver. 1.0) and PepTool (ver. 1.1), both from Biotools, and (ii) the Swiss-Prot Protein Knowledge Base (http:us.expasy.org/psrot/). Predicted topological structures of parental and modified AQP structures (PepTool) are given in Fig. 1. Exchange of corresponding N- or C-termini between AQP5 and AQP8 was accomplished using PCR-mediated gene splicing by overlap extension [15]. The final PCR products were inserted into the *Eco*RI and *Bam*HI restriction sites of the pTRE plasmid multiple cloning site. Table 1 lists cDNA fusion sites and specific deleted and replacement amino acid residues for each construct.

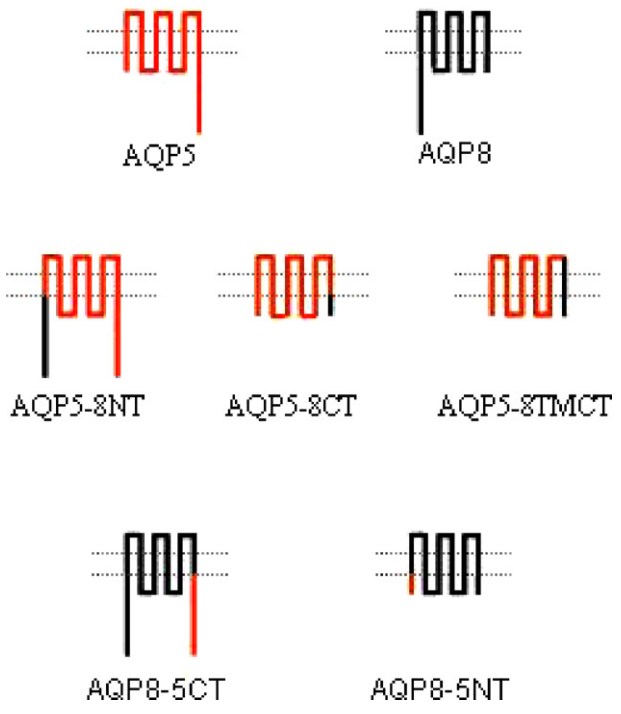

Fig. 1. Predicted membrane topologies of parental and chimeric AQPs. Parental AQPs 5 (red) and 8 (black) were used to construct chimeric AQPs as described in Materials and methods. PEPTOOL (ver. 1.1) was used to predict membrane topologies of the parental and chimeric AQPs. For each chimera, deleted and replacement amino acids are given in Table 1.

Cell culture and transfection. The culture of MDCK-II cells and the generation of stable transfectants (hygromycin-resistant) were carried out as described previously [11]. Stable transfectants were maintained in normal growth medium (hygromycin-free), and studies were conducted no sooner than one week after hygromycin removal [16]. To obtain transient transfectants for confocal microscopy, 3.4×10^5 cells/well were seeded onto Costar 24 mm polycarbonate filters (Quality Biologics), and transfections were performed 24 h later in 235 μl Optimem containing 1.9 μg of a pTRE plasmid encoding a normal or modified AQP transgene and 4.7 μl of Lipofectamine 2000 (prepared as described by Invitrogen). To obtain transient MDCK-II transfectants for Western blot analysis, transfections were performed on 10-cm dishes using 3.8×10^6 cells/plate seeded 24 h prior to transfection, and 3.3 ml/plate Optimem transfecting medium containing 26.6 μg DNA and 65.8 μl Lipofectamine 2000.

Confocal microscopy. MDCK-II parental cells or transfectants were seeded on Corning 24 mm polycarbonate filters, fixed, immunostained, and analyzed using a BioRad MRC 1024 laser scanning confocal imaging system as described previously [11]. Primary and secondary antibodies were affinity purified and used at 1:50 dilutions. Initial concentrations of primary antibodies were as follows: rabbit-anti-$AQP5_{CT}$ (0.7 mg/ml); rabbit-anti-$AQP8_{NT}$ (0.45 mg/ml); and rabbit-anti-$AQP8_{CT}$ (1 mg/ml). Rabbit-anti-$AQP5_{CT}$ (recognizes the COOH terminus of rat AQP5) and rabbit-anti-$AQP8_{NT}$ (recognizes the NH_2-terminus of rat AQP8) have been described previously [14]. Rabbit-anti-$AQP8_{CT}$ (recognizes the COOH-terminus of rAQP8) was obtained from Alpha Diagnostics. The secondary antibody (FITC)-conjugated Affinipure goat anti-rabbit IgG (H + L) (1.5 mg/ml) was purchased from Jackson ImmunoResearch Laboratories. Propidium iodide was used to detect nuclei (red).

Western blot. For each transfected construct as well as non-transfected MDCK-II cells, two 100 mm dishes of confluent cells were harvested by scraping in PBS. Crude membranes were prepared by centrifuging the cells at 3000*g* for 5 min, resuspending the pellet in lysis buffer (100 μl) containing (in mM): 100 Tris–HCl (pH 8.0), 1 $MgCl_2$, 0.5 Complete protease inhibitor containing EDTA (Roche), and 0.1 phenylmethylsulfonyl fluoride (Calbiochem), and freezing the lysate at −80 °C. The lysate was then thawed on ice, homogenized with a syringe and needle, and diluted to 1 ml with a buffer containing 0.25 M sucrose, 10 mM Tris–Hepes (pH 7.4), 1%(v/v) aprotinin, 1 mM dithiothreitol, 0.5 mM AEBSF (Roche), 0.167 mM pepstatin A (ICN Biomedicals), and 0.167 mM leupeptin (ICN Biomedicals). The lysate was centrifuged at 3000*g* for 20 min, and the resulting supernatant was centrifuged at 50,000*g* for 1 h. The resulting pellet (crude membrane fraction) was suspended in 20–30 μl water containing Complete protease inhibitor (Roche) and stored at −20 °C. The BioRad protein assay was used to measure protein concentrations. Western blots were carried out using Novex 12% Tris–glycine gels and PVDF membranes. Primary antibodies (described above) were used at a 1:1000 dilution. The secondary antibody was used as described in an Amersham ECL kit.

Transepithelial fluid movement. Measurement of osmotically obliged transepithelial fluid movement was carried as described previously [11]. Monolayer cultures grown on 24-mm polycarbonate filters were incubated in the presence of hypertonic apical medium (440 mOsm) for 30 min in a 5% CO_2 incubator at 37 °C.

Results and discussion

Here we report the effect of exchanging N- and C-termini on the localization of AQPs 5 and 8. Such exchanges might involve the gain or loss of apical or basolateral sorting determinants, potentially altering AQP localization. Results of previous studies have

Table 1
AQP constructs

Plasmid	Residues exchanged (deleted → replacement)	Fusion site
pTRE.AQP5-8CT	AQP5 F_{226}–H_{265} → I_{247}–R_{263} AQP8	TACCTGCTC/ATTAGGCTC
pTRE.AQP5-8TMCT	AQP5 H_{203}–H_{265} → F_{228}–R_{263} AQP8	AGCCCCTCT/TTCCATTGG
pTRE.AQP8-5CT	AQP8 G_{252}–R_{263} → P_{227}–H_{265} AQP5	CTCTTCATT/CCCTCCTCT
pTRE.AQP5-8NT	AQP5 M_1–K_{12} → M_1–Q_{38} AQP8	GTACATACA/AGCGGTGTT
pTRE.AQP8-5NT	AQP8 M_1–Q_{38} → M_1–K_{12} AQP5	TTCTTCAAG/CCGTGTGTG

Above is given detailed structural information regarding the AQP constructs represented schematically in Fig. 1. The deleted and replacement amino acid residues for each encoded protein are identified. In addition, the AQP chimeric cDNA transgene fusion sites are identified. Methods used to prepare the various AQP constructs are discussed in Materials and methods. The sequences of all transgene fusion sites and vector/insert joining sites were verified using an ABI 3100 Prism Genetic Analyzer.

shown that basolateral sorting signals generally dominate apical sorting signals when both signals are present in the same protein (for an exception, see [17]). Thus, when a basolateral sorting signal is lost (e.g., by deletion or mutation), the basolateral protein might sort apically due to the presence of a recessive apical sorting signal [18]. Conversely, addition of a basolateral sorting signal to an apical protein might cause redirection to the basolateral surface [19]. Altered localization might also occur if apical and basolateral sorting determinants are completely lost. In such a case, a protein might undergo stochastic partitioning to both apical and basolateral domains [5,6,12], or it might be retained and degraded in the endoplasmic reticulum [20].

Exchange of the C-termini

As shown in Table 1 and Fig. 1, the generation of the AQP5-8CT construct involved the deletion of 40 amino acids from the AQP5 C-terminus (F_{226}–H_{265}), which were replaced by 17 amino acids from the C-terminus of AQP8 (I_{247}–R_{263}). This construct was transfected into MDCK-II cells. When examined by Western blot analysis or confocal immunofluorescence microscopy, we were unable to detect AQP5-8CT expression using either transient transfectants (24–72 h post-transfection), or stable, hygromycin-resistant transfectants generated by co-transfection with pTK.Hyg (see Materials and methods).

Since we failed to detect AQP5-8CT expression, another construct, AQP5-8TMCT (Table 1 and Fig. 1), was prepared. In this construct, 63 amino acids from AQP5 (H_{203}–H_{265}) were replaced by 36 amino acids from AQP8 (F_{228}–R_{263}). This exchange involved AQP regions containing cytosolic C-termini, adjacent transmembrane regions (No. 6), and portions of extracellular E loops. As with the AQP5-8CT construct, we were unable to detect AQP5-8TMCT expression.

In contrast to results of replacing the AQP5 C-terminal regions, replacement of the C-terminus of AQP8 by the C-terminus of AQP5 resulted in a chimera that was expressed. AQP8-5CT (Table 1 and Fig. 1) was created by replacing 12 amino acids (G_{252}–R_{263}) from AQP8 with 39 amino acids (P_{227}–H_{265}) from AQP5. When crude membranes from a stable AQP8-5CT transfectant were probed with anti-rAQP-5_{CT} antibody, Western blot analysis (Fig. 2A, lane 3) revealed a lower molecular weight band corresponding to the predicted size of the non-glycosylated AQP8-5CT monomer (~31.2 kDa, 290 amino acids). As expected, AQP5 (Fig. 2A, lane 2) migrated as a smaller monomer (predicted size ~28.4 kDa, 265 amino acids). Molecular weight moieties in lane 3 larger than the ~31.2 kDa band likely represent glycosylated forms of AQP8-5CT [11,21]. Similar higher molecular weight moieties were observed in crude membranes from an AQP8 transfectant probed with either anti-AQP-8_{CT} (Fig. 2B, lane 2) or anti-AQP-8_{NT} (Fig. 2C, lane 2). As reported previously [11] and as shown in Fig. 2, we were unable to detect endogenous AQP5 (panel A, lane 1) or AQP8 (panel B, lane 1; panel C, lane 1) in crude membranes of non-transfected MDCK-II cells.

Using the anti-rAQP-8_{NT} antibody we were also able to detect the expression of AQP8-5CT by Western blot. As shown in Fig. 2 (panel C, lane 4), a band of ~31.2 kDa was detected, as were larger bands (presumably glycosylated forms of the AQP8-5CT monomer). As expected, the non-glycosylated AQP8-5CT monomer was larger than the non-glycosylated AQP8 monomer (Fig. 2C, lane 2), which migrates near its predicted size (~28 kDa, 263 amino acids).

Confocal microscopy was utilized to determine the localization of stably transfected AQP8-5CT in polarized MDCK-II monolayers. As shown in Fig. 3, when monolayers were probed with the anti-rAQP-8_{NT} antibody, examination in either the *x–z* plane (panel A) or stacked 1 μm sections in the *x–y* plane (panel B), AQP8-5CT was found localized to basolateral membranes. The same result was obtained when monolayers were probed with anti-rAQP-5_{CT}; i.e., examination of *x–z* sections (panel C) or stacked 1 μm sections in the *x–y* plane (panel D) demonstrated basolateral localization.

The results in Fig. 2D, show that AQP8-5CT was able to function as a water channel. Fluid movement across stable AQP8-5CT transfectant monolayers was significantly greater ($77 \pm 7.6\%$ greater, mean ± SEM; $P < 0.001$) than fluid movement across parental MDCK-II cell monolayers, and less than the fluid

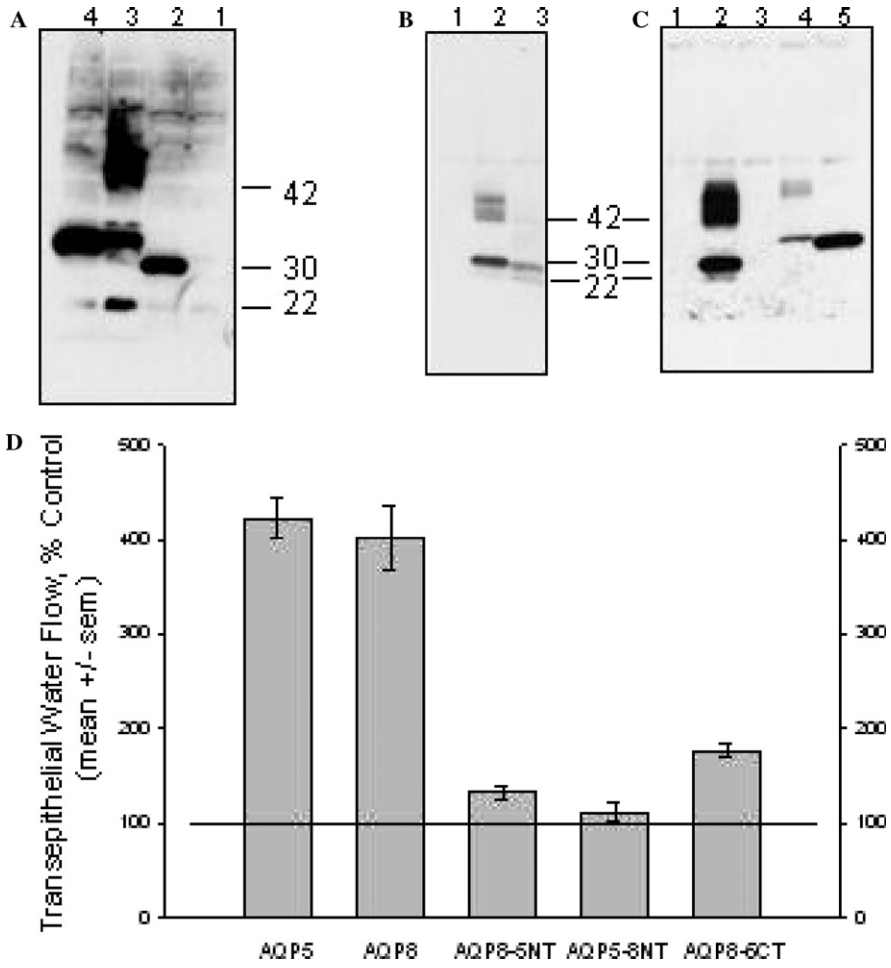

Fig. 2. Expression of AQP5, AQP8, and AQP chimeras in MDCK-II cells. (A–C) Transfections were carried out and crude membranes were prepared (Materials and methods). Each preparation (60 μg protein) was analyzed by Western blot. (A) Membranes from control MDCK-II (lane 1), AQP5 (lane 2), AQP8-5CT (lane 3), and AQP5-8NT (lane 4) transfectants probed with rabbit anti-rAQP5$_{CT}$ antibody. (B) Membranes from control MDCK-II (lane 1), AQP8 (lane 2), AQP8-5NT (lane 3) transfectants probed with rabbit anti-rAQP8$_{CT}$ antibody. (C) Membranes from control MDCK-II (lane 1), AQP8 (lane 2), and AQP8-5NT (lane 3), AQP8-5CT (lane 4), and AQP5-8NT (lane 5) transfectants probed with rabbit anti-rAQP8$_{NT}$ antibody. Indicated molecular weight markers are given in kDa. (D) Measurements of osmotically driven transcellular water flow across wild-type and stably transfected MDCK-II monolayers were carried out as described in Materials and methods. Monolayers were incubated in a hypertonic apical medium for 30 min at 37 °C in 5% CO_2. Experiments were performed in replicates of 9 (AQP5), 8 (AQP8), 12 (AQP8-5NT), 12 (AQP5-8NT), and 11 (AQP8-5CT). Matching controls (non-transfected MDCK-II cell monolayers) were also tested in each case. Results are given as percent of control for each transfectant. Osmotically driven water flow across all transfectant monolayers except AQP5-8NT was statistically different from controls (i.e., $P < 0.05$) as judged by a t test. In total, water flow across control MDCK-II cells was 1.2 ± 0.008 μl/cm^2 (mean ± SEM, $n = 54$).

movement across either AQP5 or AQP8 stable transfectant monolayers. This result might reflect: (i) intrinsic differences in AQP water channel permeabilities, (ii) differences in levels of AQP expression, or (iii) both (i) and (ii).

Exchange of the N-termini

In the AQP5-8NT construct (Fig. 1, Table 1), 12 amino acids from the N-terminus of AQP5 (M_1–K_{12}) were replaced by 38 amino acids from the N-terminus of AQP8 (M_1–Q_{38}). When crude membranes from stable transfectants were examined by Western blot analysis, the anti-rAQP-5$_{CT}$ antibody detected a band (Fig. 2A, lane 4) that migrated near the predicted size of the AQP5-8NT monomer (~31.5 kDa, 291 amino acids). The anti-rAQP-8$_{NT}$ antibody also detected a band that migrated near the predicted size of the AQP5-8NT monomer (Fig. 2C, lane 5). A comparison of lanes 2 and 4 (Fig. 2A) shows that, as expected, the size of AQP5-8NT was larger than AQP5 (~28.4 kDa, 265 amino acids).

As shown in Fig. 4, the localization of the AQP5-8NT construct was different from parental AQP5, which sorts apically in polarized MDCK-II cells [11]. Examination in the x–z plane (Fig. 4A) or in stacked 1 μm sections in the x–y plane (Fig. 4B) shows that the anti-rAQP-5$_{CT}$ probe did not detect AQP5-8CT localized

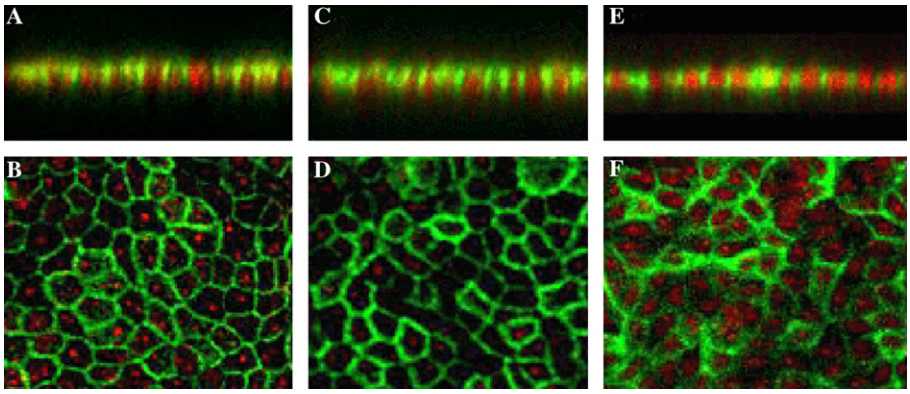

Fig. 3. Localization of AQP8-5CT and AQP8-5NT. Stable transfectants were grown as polarized monolayers on polycarbonate filters. Cells were fixed, incubated with appropriate antibodies and propidium iodide, and examined by confocal immunofluorescence microscopy. (A,C) AQP8-5CT *x–z* sections; (B,D) AQP8-5CT 1 μm sections stacked in the *x–y* plane. (E) AQP8-5NT *x–z* section. (F) AQP8-5NT 1 μm sections stacked in the *x–y* plane. (A,B) Monolayers probed with the primary antibody rabbit anti-rAQP8$_{NT}$; (C,D) Monolayers probed with the primary rabbit antibody anti-rAQP5$_{CT}$; and (E,F) Monolayers probed with the primary antibody rabbit anti-AQP8$_{CT}$. FITC-goat anti-rabbit IgG (H + L) served as the secondary antibody.

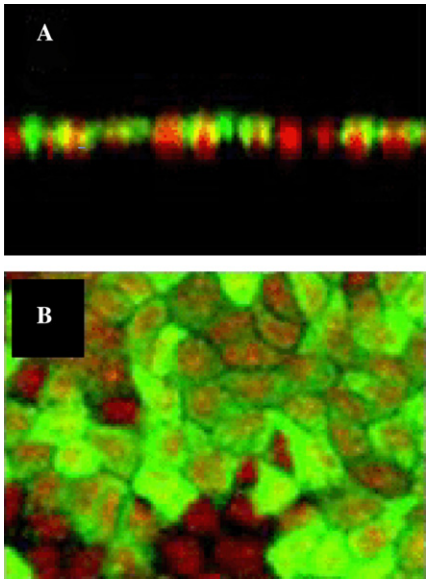

Fig. 4. Localization of AQP5-8NT. Experiments were carried out as described in the legend to Fig. 3, using an AQP5-8NT stable transfectant. (A) *x–z* section; (B) 1 μm sections stacked in the *x–y* plane. The monolayer was probed with the primary antibody rabbit anti-rAQP5$_{CT}$. FITC-goat anti-rabbit IgG (H + L) served as the secondary antibody.

to apical membranes. Rather it appears that this construct was trapped in intracellular structures. Furthermore, results in Fig. 2D demonstrate that osmotically obliged transepithelial fluid movements across parental MDCK-II and stable AQP5-8NT monolayers were not significantly different ($P = 0.285$). Our failure to detect facilitated transepithelial fluid movement by AQP5-8NT might have resulted from: (i) a loss of water channel function, (ii) lack of AQP5-8NT expression at the plasma membrane, or (iii) both (i) and (ii).

In the AQP8-5NT construct (Table 1 and Fig. 1), a 12 amino acid sequence from AQP5 (M_1–K_{12}) replaced a 38 amino acid sequence in AQP8 (M_1–Q_{38}). When probed with anti-AQP-8$_{CT}$ antibody, a band near the predicted size of the monomer (~25 kDa, 237 amino acids) was detected in crude membranes from a stable transfectant (Fig. 2B, lane 3). This band was slightly smaller than AQP8 (compare lanes 2 and 3), which has a predicted size of ~28 kDa (263 amino acids). As expected, we did not detect a band using the anti-AQP-8$_{NT}$ probe (Fig. 2C, lane 3).

Confocal analysis was performed on polarized monolayers of the stable AQP8-5NT transfectant. When probed with anti-AQP-8$_{CT}$, AQP8-5NT was localized to basolateral membranes when viewed in the *x–z* plane (Fig. 3E) and in stacked 1 μm sections in the *x–y* plane (Fig. 3F). Thus, this modification of of the N-terminus of rAQP8 did not alter basolateral localization in MDCK-II cells.

Results shown in Fig. 2D demonstrate that fluid movement across AQP8-5NT transfectant monolayers was significantly greater (34 ± 8.3% greater, mean ± SEM; $P = 0.013$) than that across non-transfected MDCK-II cell monolayers, indicating that this construct possesses at least some of the functional properties of an AQP water channel. As with the result concerning AQP8-5CT, however, this increase in fluid movement was considerably less than that observed across AQP5 or AQP8 transfectant monolayers, perhaps due to differences in AQP permeabilities and/or levels of expression.

Summary

The modified AQP5 constructs studied here were either not detectable or did not display a typical apical

or basolateral localization pattern, such as those displayed by native AQP5 and AQP8, respectively [11]. These constructs might have been unstable or mistargeted due to protein misfolding and a disruption of tetramer formation. In contrast, our modifications of both the N- and C-termini of AQP8 were stably expressed, facilitated osmotically obliged transepithelial fluid transport, and localized to the basolateral membranes of MDCK-II cells. The failure of cytosolic termini modifications to affect AQP8 basolateral localization suggests that either a basolateral signal is not located in the termini of AQP8 or that a basolateral signal was added to AQP8 from a replacement AQP5 terminus. While we cannot rule out the latter possibility, it seems unlikely. As stated previously, basolateral sorting signals usually dominate apical sorting signals when both are present in the same protein, suggesting, therefore, that AQP5 probably does not possess a basolateral sorting signal. Thus, the most likely explanation for our failure to change AQP8 basolateral localization is that, unlike the AQP2 and AQP4 targeting/retention signals reported previously, the AQP8 basolateral targeting/retention signal lies between the N- and C-cytosolic termini. Further experiments will be required to either confirm or deny this possibility.

References

[1] M. Ikeda, E. Beitz, D. Kozono, W.B. Guggino, P. Agre, M. Yasui, Characterization of aquaporin-6 as a nitrate channel in mammalian cells, J. Biol. Chem. 277 (2002) 39873–39879.

[2] P. Agre, L.S. King, M. Yasui, W.B. Guggino, O.P. Ottersen, Y. Fujiyoshi, A. Engel, S. Nielsen, Aquaporin water channels—from atomic structure to clinical medicine, J. Physiol. 542 (2002) 3–16.

[3] A.S. Verkman, A.K. Mitra, Structure and function of aquaporin water channels, Am. J. Physiol. Renal Physiol. 278 (2000) F13–F28.

[4] M. Borgnia, S. Nielsen, A. Engel, P. Agre, Cellular and molecular biology of the aquaporin water channels, Annu. Rev. Biochem. 68 (1999) 425–458.

[5] T.R. Muth, M.J. Caplan, Transport protein trafficking in polarized cells, Annu. Rev. Cell Biol. 19 (2003) 333–366.

[6] D. Brown, S. Breton, Sorting proteins to their target membranes, Kidney Int. 57 (2000) 816–824.

[7] E.J. Kamsteeg, D.G. Bichet, I.B.M. Konings, H. Nivet, M. Lonergan, M.F. Arthus, C.H. van Os, P.M.T. Deen, Reversed polarized delivery of an aquaporin-2 mutant causes dominant nephrogenic diabetes insipidus, J. Cell Biol. 163 (2003) 1099–1109.

[8] M-P. Stein, A. Wandinger-Ness, T. Roitback, Altered trafficking and epithelial cell polarity in disease, Trends Cell Biol. 12 (2002) 374–381.

[9] S. Steinfeld, S.S. Cogan, L.S. King, P. Agre, R. Kiss, C. Delporte, Abnormal distribution of aquaporin-5 water channel protein in salivary glands from Sjogren's syndrome patients, Lab. Invest. 81 (2001) 143–148.

[10] E.M. Fish, B.A. Molitoris, Alterations in epithelial polarity and the pathogenesis of disease states, N. Engl. J. Med. 330 (1994) 1580–1588.

[11] R.B. Wellner, B.J. Baum, Polarized sorting of aquaporins 5 and 8 in stable MDCK-II transfectants, Biochem. Biophys. Res. Commun. 285 (2001) 1253–1258.

[12] B.W.M. van Balkom, M.P.J. Graat, M. van Raak, E. Hoffman, P. van der Sluijs, P.M.T. Deen, Role of cytoplasmic termini in sorting and shuttling of the aquaporin-2 water channel, Am. J. Physiol. Cell Physiol. 286 (2003) C372–C379.

[13] R. Madrid, S. LeMaout, M.-B. Barrault, K. Janvier, S. Benichou, J. Merot, Polarized trafficking and surface expression of the AQP4 water channel are coordinated by serial and regulated interactions with different clathrin–adaptor complexes, EMBO J. 20 (2001) 7008–7021.

[14] R.B. Wellner, A.T. Hoque, C.M. Goldsmith, B.J. Baum, Evidence that aquaporin-8 is located in the basolateral membrane of rat submandibular gland acinar cells, Pflügers Arch. 441 (2000) 49–56.

[15] A.N. Vallejo, R.J. Pogulis, L.R. Pease, Mutagenesis and synthesis of novel recombinant genes using PCR, in: C.W. Dieffenbach, G.S. Dveksler (Eds.), PCR Primer, A Laboratory Manual, Cold Spring Harbor Press, Plainview, NY, 1995, pp. 603–612.

[16] A. Rodolosse, A. Barbat, I. Chantret, M. Lacasa, E. Brot-Laroche, A. Zweibaum, M. Rousset, Selecting agent hygromycin B alters expression of glucose-regulated genes in transfected Caco-2 cells, Am. J. Physiol. Gastrointest. Liver Physiol. 274 (1998) G931–G938.

[17] R. Jacob, U. Preuss, P. Panzer, M. Alfalah, S. Quack, M.G. Roth, H. Naim, Hierarchy of sorting signals in chimeras of intestinal lactase-phlorizin hydrolase and the influenza virus hemagglutinin, J. Biol. Chem. 274 (1999) 8061–8067.

[18] W. Hunziker, C. Harter, K. Matter, I. Mellman, Basolateral sorting in MDCK cells requires a distinct cytoplasmic domain determinant, Cell 66 (1991) 907–920.

[19] L.S. Nadler, G. Kumar, N.M. Nathanson, Identification of a basolateral sorting signal for the M_3 muscarinic acetylcholine receptor in Madin–Darby canine kidney cells, J. Biol. Chem. 276 (2001) 10539–10547.

[20] L. Elgaard, A. Helenius, ER quality control: towards an understanding at the molecular level, Curr. Opin. Cell Biol. 13 (2001) 431–437.

[21] F. Garcia, A. Kierbel, M.C. Larocca, S.A. Gradilone, P. Splinter, N.F. LaRusso, R.A. Marinelli, The water channel aquaporin-8 is mainly intracellular in rat hepatocytes, and its plasma membrane insertion is stimulated by cyclic AMP, J. Biol. Chem. 276 (2001) 12147–12152.